



<http://www.diva-portal.org>

Postprint

This is the accepted version of a paper presented at *The 18th International Nondestructive Testing and Evaluation of Wood Symposium, September 24-27, 2013, Madison.*

Citation for the original published paper:

Hu, M., Johansson, M., Olsson, A., Enquist, B. (2013)

Comparison of local variation of modulus of elasticity determined on basis of scanned fiber angles and full strain field measurements.

In: (ed.), *The 18th International Nondestructive Testing and Evaluation of Wood Symposium*
Madison, WI, USA

N.B. When citing this work, cite the original published paper.

Permanent link to this version:

<http://urn.kb.se/resolve?urn=urn:nbn:se:lnu:diva-30468>

Comparison of local variation of modulus of elasticity determined on basis of scanned fiber angles and full strain field measurements

Min Hu

Department of Building and Energy Technology, Linnaeus University, Sweden, Email: min.hu@lnu.se

Marie Johansson

Department of Building and Energy Technology, Linnaeus University, Sweden, Email: marie.johansson@lnu.se

Anders Olsson

Department of Building and Energy Technology, Linnaeus University, Sweden, Email: anders.olsson@lnu.se

Bertil Enquist

Department of Building and Energy Technology, Linnaeus University, Sweden, Email: bertil.enquist@lnu.se

Abstract

Laser scanning of fiber angles has shown to be a powerful tool to establish bending MOE profiles along boards. This study aims at investigating the accuracy of the MOE variation determined on basis of fiber angles obtained from laser scanning. Material employed was a board of Norway spruce of dimension 50×150×3900 mm. Firstly fiber angles on four surfaces were identified using a WoodEye scanner and based on the fiber angles the MOE profile which was calibrated according to the longitudinal resonance frequency was established. Thereafter the board was subjected to bending and during loading an image correlation system, ARAMIS, was engaged to detect the strain field. Subsequently the strain field was used to obtain the MOE variation. The MOE profiles determined in two different ways were compared and they showed close compliance. However, differences were found as well. The research thus contributes to further improvement of a newly suggested grading method.

Keywords: Finite element analysis, Strength grading, Fiber angle scanning, Strain field, Image correlation

1. Introduction

Most strength grading machines on the European market are based on the relationship between a measured MOE for each board and the bending strength. An assumption often made is that the measured MOE is valid for the whole board. In reality, knots and other defects cause large variation in stiffness along boards and if this variation could be taken into account better predictions of strength could be reached. Many studies have shown that with better knowledge of local variation of the MOE, a higher coefficient of determination (R^2) with respect to bending strength could be obtained (e.g. Isaksson 1999). In this context, measurement of fibre angles using laser scanning has shown to be a powerful tool. As wood is a strongly orthotropic material, with high stiffness in the fibre direction, deviation in fibre orientation around for example knots causes considerable reduction in the bending stiffness. With knowledge of fibre orientation from laser scanning it is thus possible to calculate a bending stiffness profile along an individual board. Moreover, this can be done at a speed

corresponding to the production speed at sawmills and hence it can be utilized for commercial strength grading purposes.

The aim of the present study is to study the MOE profile established based on full-field displacement measurement along a board during a bending test and compare this profile with the MOE profile based on fibre angles from laser scanning as suggested by Olsson et al. (2013). A 3D non-contact deformation measurement system ARAMIS® was employed to capture the displacement field of one surface of a board exposed to pure bending. The displacements were detected at known stress levels and therefore a MOE profile could be established and compared with the one established on basis of fibre orientation information.

2. Material

A board of Norway spruce was chosen for the study from a sample collected from southern Sweden. The choice was made because of the board's relatively large defects/knots and distinct weak sections along the longitudinal board direction. Dynamic test has been carried out on this board earlier (Hu et al. 2011), and the dynamic MOE (cf. Table 1) in accordance with the first axial natural frequency has been registered. The relevant material properties are found in Table 1. Before the tests, the board was conditioned in a climate room with a temperature of 20°C and a relative humidity of 65%.

Table 1--The relevant material parameters of the specimen.

Material parameter	Value
Dimension	50×150×3900 mm
Density	454kg/m ³
1 st axial frequency	637Hz
Dynamic MOE	10.98GPa

3. Method and measurements

The laboratory measurements provided data of 1) 3D coordinates on one surface of the board before and after deformation and 2) fiber angles on four surfaces of the board. The test set up and measuring procedures are further described below. In addition to the laboratory tests, the study also comprises numerical calculation and FE modeling which were implemented using the software MATLAB/CALFEM®.

3.1 Strain measurement on board subjected to static bending

As mentioned before, an image correlation system ARAMIS was used to capture the deformation field along the board. ARAMIS is a contact free measuring system which provides 3D surface coordinates. It recognizes surface structure of the studied object in digital camera images and allocates coordinates to image pixels. ARAMIS records images before, during and after deformation and the first image recorded represents the undeformed state. The recorded digital images are applied for calculating the deformations (GOM 2009).

To facilitate a constant bending moment along the whole board, for creating a MOE profile based on the strain measurements, the board was lengthened by finger jointing an extra 550 mm long board at each end of the original board (cf. Figure 1). The bending test as sketched in Figure 1 was arranged as four-point bending where the board was symmetrically loaded at two points over a span of 3900 mm. In such a case, the mid span i.e. the whole original board was exposed to a pure constant bending moment without shear. The board was loaded at five different load/stress levels, i.e. five load stages were applied, and the corresponding load/stress level of each load stage are reported in Table 2. To record deformation along the whole mid span, twelve ARAMIS projects, each covering a measuring area of 480 × 480 mm on the object surface, were created along the board for each load stage. This gave a resolution of the ARAMIS measurement that was approximate 3 mm in both *x*- and *y*-direction. With the aid of another contact free measurement system, TRITOP, the twelve separate

ARAMIS projects were combined into one project sharing a global coordinate system (Oscarsson 2012).

Table 2 The load stages of ARAMIS measurement.

Stage no.	0	1	2	3	4
Nominal load F [kN]	0.5	2.0	4.0	5.5	7.0
Nominal stress σ [MPa]	1.5	5.9	11.7	16.1	20.5

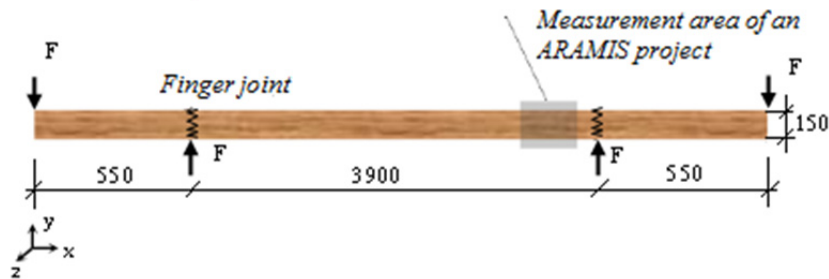


Figure 1 Four point bending test setup, length unit [mm].

3.2 Fiber angle detection using a WoodEye scanner

A WoodEye scanner from Innovative Vision AB was used to detect the fiber angles on the board surfaces. A WoodEye scanner is mainly equipped with four sets of multisensor cameras, dot and line lasers and conveyor belts. To detect the fiber orientation on wood surfaces it utilizes the so called tracheid effect which means that the most extended principal axis of light intensity distribution around a laser dot is oriented in the direction of the fiber. Figure 2 shows an example how the fiber directions on a wood surface are identified using the tracheid effect. The photograph to the left shows a wood surface including a knot; the middle image shows how the light from dot lasers spread on the wood surface and the right plot displays the identified fiber orientation. The local fiber angles on four surfaces of a wooden board are registered when a board is fed through the scanner. The resolution employed for the scanning data, i.e. the distance between laser dots, is 0.8 mm in x - direction (along the board) and 3.6 mm in y - direction (across the board, cf. Figure 1). For further information regarding the WoodEye scanner, reference is made to Olsson et al. (2013).

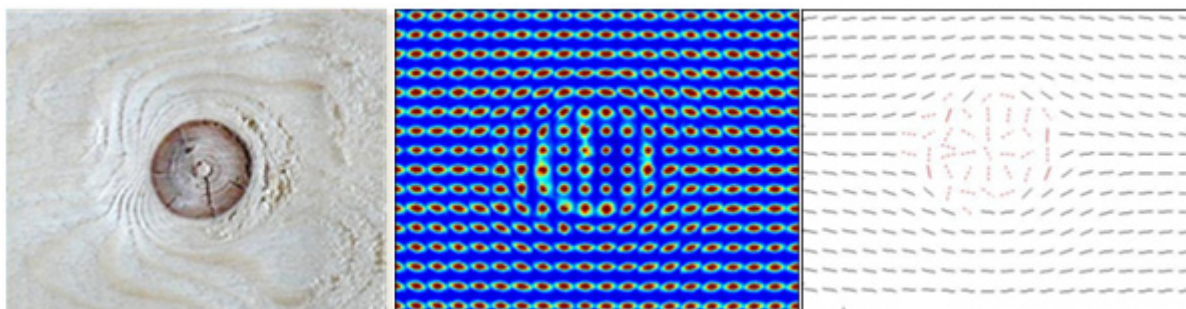


Figure 2 A wood surface containing a knot (*left*); an image illustrating the tracheid effect (*middle*); the fiber orientation on the wood surface identified by utilizing the tracheid effect (*right*) (Olsson et al 2013).

3.3 Calculation of bending MOE based on ARAMIS data

The displacement data from ARAMIS of load stage 1 and 4, of which the nominal normal stress levels are 5.9 MPa and 20.5 Mpa, respectively, was used to establish the MOE profile. The calculation was carried out as follows:

- The object surface was divided into small rectangular subareas which conformed to the spatial resolution of the ARAMIS displacement data, and the data was rearranged in the form of a matrix. Each column/row in the matrix represented data points located on one vertical/horizontal line. In addition, each column of subrectangulars as a whole was regarded as a 'section' representing an unique position in x - direction.

- The relative displacements of adjacent data point were used to calculate strains. However, the so calculated strain field includes a lot of noise, cf. Figure 3 (top).
- To suppress the noise, a smoothing function was applied. It calculates the average strain over a selected surrounding area and assigns the average value to the subrectangular in question. The strain field after smoothing is shown in Figure 3 (down), where the average value is calculated over an area of 12×12 mm.
- Thereafter, a linear regression line for the strains of each section was estimated, and the position of the neutral layer, denoted \bar{y} , was set to coincide with the y coordinate where the linear strain achieved the value of zero. The linear regression of two selected sections are shown in Figure 3 to provide a general idea of how well the regression models fit the calculated strains. In accordance with Euler-Bernolli beam theory, the bending stiffness EI of each section was obtained as:

$$EI = \frac{M(y_m - \bar{y})}{\varepsilon_m} \quad (1)$$

where M is the bending moment, y_m and ε_m is a y coordinate and the corresponding strain value, respectively, on the line of regression. The EI profile for the whole board was obtained by considering EI values of all sections along the board.

- At last, the bending MOE profile was obtained as:

$$MOE = \frac{EI}{I_h} \quad (2)$$

where I_h is the nominal second moment of inertia. Note that it is dependent only on the dimension of the cross section.

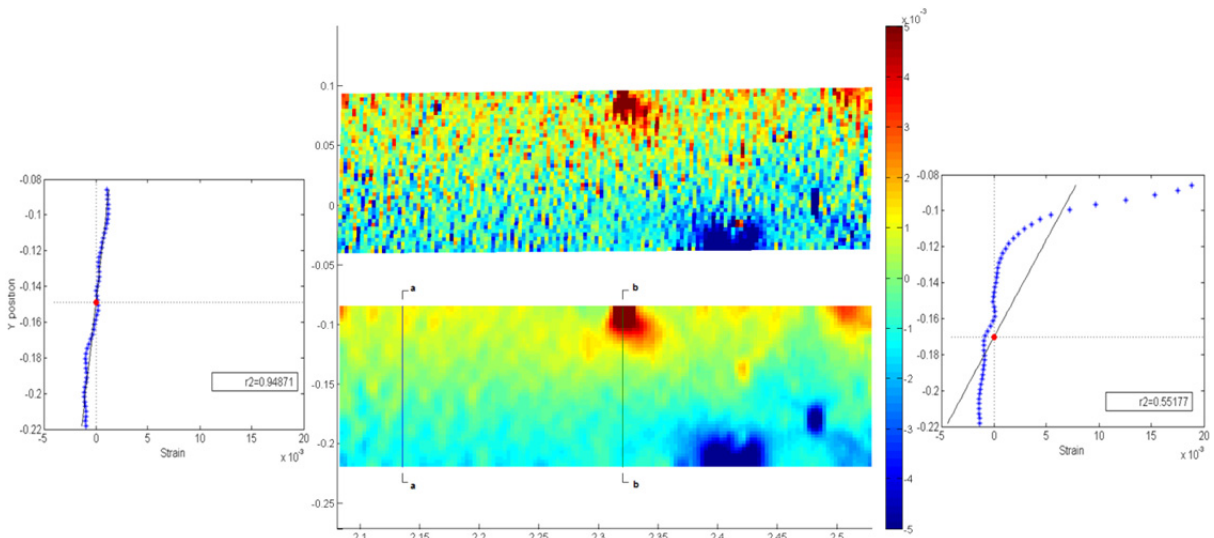


Figure 3 Illustration of the effect of the smoothing function and the linear regression implemented on the smoothed strains. The middle part shows color plots of strains in the longitudinal direction of the board calculated on basis of an ARAMIS project before (*top*) and after (*down*) application of the smoothing function. The graphs at both sides show the scatter plot of the smoothed strains and the corresponding regression line for section *a-a* (*left*) and *b-b* (*right*). The red dots in the graphs indicate the position of the neutral axes. r^2 values displayed are the coefficients of determination of the regression model.

3.4 Calculation of bending MOE on basis of fiber angle

Olsson et al. (2013) suggests a scheme for calculating bending MOE profile based on the fiber angles and shows that rather accurate prediction of bending strength can be performed on basis of such profiles. In the method presented four surfaces of boards are scanned with dot lasers in a WoodEye scanner. Transformations taking material properties in different directions into account give basis for calculation of local material stiffness in board direction which in turn gives basis for establishing a MOE profile valid for bending. Important assumptions in the method are that: a) density (ρ) and the MOE in the fiber direction (E_l) are constant within a board, b) other stiffness parameters than E_l are linear functions of E_l , c) fiber angles detected on surfaces are located in the l - r plane, d) the fibers are

oriented in a plane which coincide with the wood surfaces, i.e. the so called diving angles are assumed to be zero and e) the fiber angles detected on a surface are representative for the fiber orientation to a certain depth within the board. Thus, except the density ρ , which is determined as the mass of the board divided by its volume, the only parameter that has to be determined individually for each board is E_l . This parameter is determined by an eigenfrequency analysis on a simple finite element beam model. The model employs the transformed MOE variation along the board and E_l is obtained by achieving the same natural frequency from the model as the one determined experimentally. The steps taken to calculate the MOE profile can be described as follows:

- The fiber orientation in each data point with spatial resolution of 0.8×3.6 mm is calculated.
- The material properties are transformed from the local direction to the board direction, whereby particularly the material stiffness in the longitudinal direction of the board, $E_x(x,y)$, is calculated.
- The global bending stiffness based on the transformed MOE variations are used in a simple finite element model for an eigenfrequency analysis to achieve the same resonance frequency as the one determined experimentally, whereby the value of E_l and accordingly $E_x(x,y)$ get calibrated for the particular board in study.
- By applying assumption e) mentioned above, i.e. that for a given position (x, y) , a same value of E_x applies over a certain thickness (in z - direction), the cross-sectional bending stiffness with respect to z - axis could be calculated as:

$$EI = \iint E_x (y - \bar{y})^2 dA \quad (3)$$

- Finally, the bending MOE for each position along the board was obtained as:

$$MOE = \frac{EI}{I_h} \quad (4)$$

where I_h is the nominal second moment of inertia which is dependent only on the dimension of the cross section.

For a more detailed description of the procedure, reference is made to Olsson et al (2013).

4. Results and discussions

The MOE profiles estimated from the strain and fiber angle measurements, with their respective maximum resolution, as well as an image of the four surfaces of the actual board are shown as the top part of Figure 4. In the full resolution plot despite the rippled pattern observed on both curves, which is due to the high resolution and noise, it appears that the weak sections according to calculated MOE profiles based on fibre angle data from WoodEye and from strains detected by ARAMIS, respectively, are closely correlated. To even out some of the noise, 80 mm moving average of the MOE is performed and the resulting curves are presented as the second plot of Figure 4. When comparing the curves with the board image it is found that the MOE profiles drop at positions where knots are observed on the board surface. Based on different methods a mean value of the MOE for the whole board can be calculated (cf. Table 3). It should be noted that the mean MOE calculated from ARAMIS strain is given as a range which is due to the load uncertainty during the measurement. As stated earlier, it was necessary to move the cameras along the board and create twelve ARAMIS projects to cover the whole S2 surface and for each load stage this process took 30 minutes. We aimed at applying a constant load, but some variation in the applied load level could not be avoided. Overall the load level of each stage might vary ± 200 N which corresponds to ± 0.97 GPa in the estimated MOE. At this point, small discrepancies are found for the mean values of evaluated MOE presented in Table 3.

Table 3—The mean value of MOE based on the the first longitudinal resonance frequency, the fiber angle data and the strain(in x - direction) measurements respectively.

Method	Resonance frequency	Fiber angle	Strain
Mean MOE [GPa]	10.98	11.32	12.20 \pm 0.97

The color image in the middle of Figure 4 shows the strain field in x - direction of S2 which indicates compressive strains at the top and tension strains at the bottom. It is also possible to observe strain concentrations around knots which are visible on the wood surface. As shown in Figure 4, regarding the position of weak sections and the absolute value, some parts of two curves end up with a very good agreement and some parts do not. One discrepancy can be seen in the left part of the curves where the MOE based on strain data gives a higher maximum level than the one based on fiber angles. The model based on fiber angles assumes a constant E_l along the whole board which for this particular board is probably not true. The higher mean MOE in the left end of the tree pointed out by the ARAMIS strain result might be caused by the growth conditions for the tree.

For the individual drops in the curves it is also possible to see very good agreement in some positions and worse agreement in other positions. This is related to the calculation model and to the type of knot groups present in different sections. Typical examples for two different type of knot groups are shown by the highlighted zones, A and B, at the bottom of Figure 4. In the longitudinal board direction, the knots in zone A are spread out, whereas knots in zone B are positioned in a narrow band.

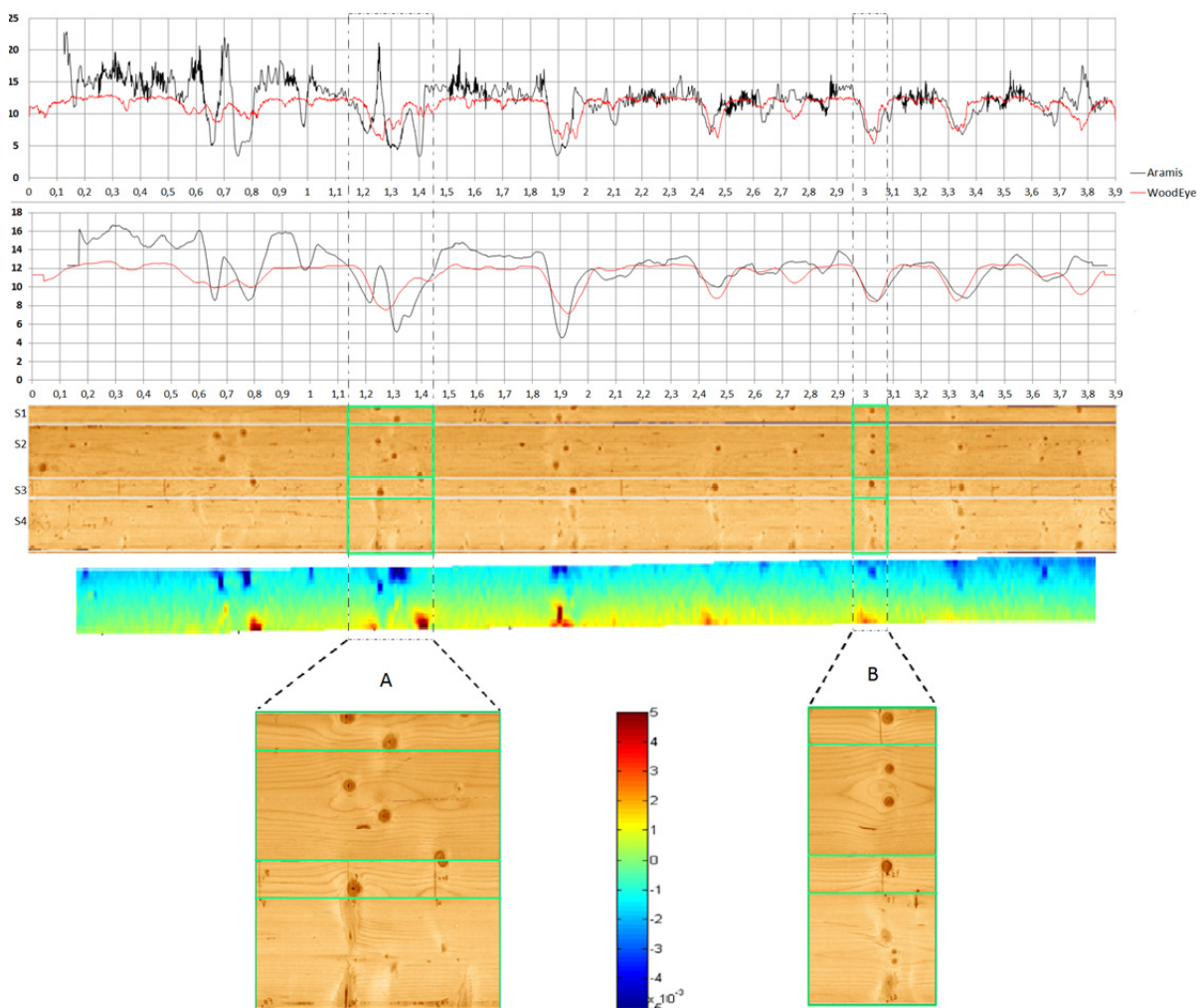


Figure 4— Diagrams of the estimated MOE profiles based on fiber angle scanning and strain measurements (denoted “WoodEye” and “ARAMIS”, respectively), photographs of the board surfaces and the estimated x - strain based on ARAMIS data. *Key:* the top two diagrams show MOE variation with the maximal resolution (*up*) and with a resolution of 80 mm (*down*). The middle parts show the photographs of all four surfaces marked as S1~S4 of the board, extracted from the WoodEye scanner. The next plot shows the strain field on the S2 surface after the smoothing function is applied, and the color scale employed is shown below. The two pictures at bottom illustrate the enlargement of two segments of the board surfaces.

Zone A thus contains a knot cluster that is spread out over 150 mm in longitudinal board direction while zone B embraces a knot cluster that is well collected in longitudinal direction. On the lower edge of the strain image large tension strains can be detected even without knots visible on the S2 surface. This is an influence of the knot which is visible on the S3 surface. It shows that based on strains measured on only one surface of the board the strains detected using ARAMIS system is capable of capturing the weaknesses in the board which are not visible on the surface in study. The same effect can also be observed for zone A where the knots on S1 and S3 have an influence on the strains field of S2. For zone B the MOE profiles calculated based on both strain and fiber angle data show the same minimum value at the same location. All the knots in zone B are located almost at the same position in the longitudinal board direction. Therefore a very good agreement on position is obtained. For zone A different patterns of the two MOE profiles are found. Two sharp drops appear in the ‘ARAMIS profile’ but only a single drop in the ‘WoodEye profile’. The knots in zone A is more spread out in the longitudinal direction. When we look at the strain pattern it is possible to see that there are large effects of knots at two sections corresponding to the two drops in the ‘ARAMIS profile’. While the laser scanning measurement shows disturbances in the fiber angles in the area between the knots which result in one wide flat drop in the MOE profile.

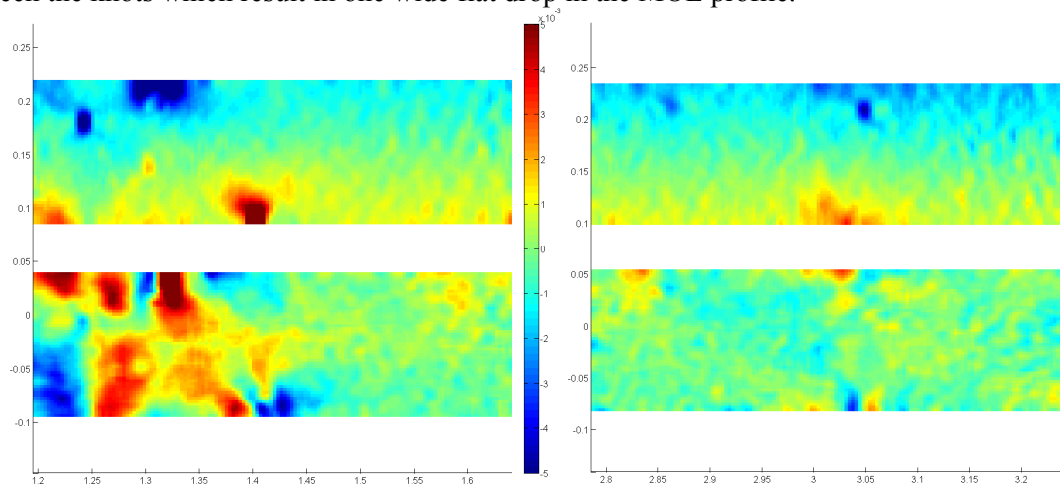


Figure 5- The x strains (*up*) and shear strains (*down*) around knot cluster in zone A (*left*) and B (*right*).

As mentioned above ARAMIS system measures 3D deformation, thus it is possible to study the shear strains. Referring to Figure 5 although the pure bending according to Euler-Bernoulli beam theory which should result in very small shear, it is obvious that large shear deformations occurred in the material. The shear strains are especially visible around knot cluster A. For knot cluster B, i.e. with knots in a group are located along a vertical line perpendicular to the longitudinal board direction, the occurring deformations are such that they can be properly modeled with the beam theory. While the knots in a group are more spread out in the longitudinal direction, however, large shear strains occur due to irregularities in the material directions and properties, which cannot be fully captured by the beam theory and thus the calculated bending stiffness overestimates the true local stiffness.

5. Conclusions

Only one surface of the board was examined by ARAMIS and the strain field detected depends, on a local scale, very much on the knots visible on the examined surface. Therefore a high resolution MOE profile, calculated on basis of the strain field detected of one surface of the board, would differ from a MOE profile calculated on basis of the strain field of the other surface. On a more global level, however, information from just one surface of the board for evaluation of bending stiffness should be sufficient since the curvature of the board, except on a very local scale, is almost equal on the two sides of the board in bending. Thus the reliability of a MOE profile, calculated using the strain data of only one surface, depends on the scale considered. Whether the scale corresponding to the 80 mm moving average employed in the present analysis represents a resolution that is coarse enough or not

in this respect may be questioned. Having this kept in mind, good agreement regarding the position and magnitude of weak section is obtained where a group of knots are clustered more closely together in longitudinal board direction while it becomes worse where a group of knots is more spread out in longitudinal direction. The MOE profile established on basis of fiber angles from laser scanning in the way described shows an overall good agreement with the MOE profile established on basis of strains detected by ARAMIS. Therefore the present research supports conclusions drawn in previous research, namely that MOE profiles established on basis of fibre angle information in the way described may be used for rather accurate strength prediction of boards. The present research also reveals, however, that the local stiffness, in regions with clusters of knots spread out in longitudinal board direction, can not be properly captured by the beam theory that the method employs. This conclusion should be the starting point for further development of the method towards improved measures of local stiffness leading to even more accurate predictions of bending strength.

References

- T. Isaksson (1999). Modeling the variability of bending strength in structural timber – Length and load configuration effects. Division of structural engineering, Lund Institute of Technology.
- A. Olsson, J. Oscarsson, E. Serrano, B. Källsner, M. Johansson and B. Enquist (2013). Prediction of timber bending strength and in-member cross-sectional stiffness variation on basis of local wood fiber orientation. *European Journal of Wood and Wood Products*. DOI 10.1007/s00107-013-0684-5.
- M. Hu, M. Johansson, A. Olsson, C. Bengtsson and A. Brandt (2012) Grading of sawn timber using the vibration technique - Locating imperfections based on flexural mode shapes. 17th international nondestructive testing and evaluation of wood symposium. 269-276.
- H. Petersson (2010). Use of Optical and Laser Scanning Techniques as Tools for Obtaining Improved FE-input Data for Strength and Shape Stability Analysis of Wood and Timber. IV European Conference on Computational Mechanics, May 2010, Paris.
- GOM mbH (2007) ARAMIS User manual- Software, Version 6.1 and higher.
- J. Oscarsson (2012), Strength grading of structural timber and EWP laminations of Norway spruce- Development potentials. Licentiate thesis, school of engineering, Report No.15, Linnaeus university, Växjö, Sweden.
- S. Ormarsson (1999) Numerical Analysis of Moisture-Related Distorsions in Sawn Timber. Doctoral thesis, Chalmers University of Technology, Gothenburg.
- J. M. Dinwoodie (2000) Timber: Its nature and behavior. E & FN Spon, New Fetter Lane, London.